ACOUSTICS 2012

Prediction of structure-borne vibration for an assembly of three structures in series

M.-H. Moulet[a,b] and V. Martin[c]

[a]Laboratoire d'acoustique de l'université du Maine, Bât. IAM - UFR Sciences Avenue Olivier Messiaen 72085 Le Mans Cedex 9
[b]Centre de Transfert de Technologie du Mans, 20 rue Thalès de Milet, 72000 Le Mans, France
[c]CNRS, UMR CNRS/UPMC 7190, Institut Jean Le Rond d'Alembert, 75005 Paris, France
marie-helene.moulet@univ-lemans.fr

The prediction of structure-borne sound and vibration in an assembly of two structures needs the prediction of the forces applied by the source structure on the host or receiver structure. Often, the source structure excites the receiver through an intermediary structure. Two ways are possible to describe three structures in series: by creating a new receiver as the assembly of the intermediary and receiver structures or by creating a new source as the assembly of intermediary and source structures. In the present paper, two methods used to calculate forces entering the host structure are presented. Results in an industrial case show that the prediction of forces for three structures in series is better when based on inertance measurements of certain coupled structures rather than of isolated structures. In order to understand which degrees of freedom are linked in the previous case, a numerical bench is developed. The first step of validation concerns the coupling of two beams.

1 Introduction

In a lot of engineering situations, a source structure excites a host or receiver structure through an intermediary structure. To understand how the receiver structure will radiate, forces entering the host structure have to be evaluated. When the host structure is known only by its specifications, the assembly of the three structures is not possible: forces can be predicted from measurements on a test bench.

To describe three structures in series, two approaches are possible: the first one consists in creating a new receiver as the assembly of the intermediary and the receiver structures and the second one consists in creating a new source as the assembly of the source structure and the intermediary one. In this paper, we consider that no physical couplings are possible between the intermediary and the receiver structures as well as between the source and the intermediary ones. However, two different methods are presented: in the first one, called standard method, the characteristics of a new receiver are found from measurements of isolated structures and in the second one, called alternative approach, the characteristics of a new source are found from measurements of isolated structures and two coupled structures : the intermediary and the bench structures. Experimental results are presented for these two methods in the case of a fan system in a car. These results are based on work presented in [1].

The second part deals with a numerical bench: the aim of this bench will be to validate in an academic case the results obtained with the previous two methods in a complex case. As a first step, this numerical bench is validated for two coupled beams in the present paper. The results presented here are based on work in [2].

2 Recall of two methods to couple three structures in series

2.1 Nomenclature and generic configuration

The generic configuration is given in Figure 1. We consider a source structure Ω^A coupled to a virtual host structure Ω^C through an intermediary structure Ω^F. The source is submitted to an excitation while the two others are passive. The links between these three structures can be elastic and/or rigid [3]: the links between Ω^A and Ω^F, respectively between Ω^F and Ω^C, constitute a structure named $\Omega^{K'}$, respectively Ω^K. The objective is to predict f_a^C, the forces entering the host structure Ω^C, from measurements of forces f_a^B measured on a rigid bench Ω^B (Figure 1 (b)).

If we consider a structure Ω^H, connections with other structures will occur at some points on the boundary differentiated by the letters *a* and *b*, the former are called input points, the latter output points. In all figures, the measured parameters as inertance matrices or force vectors are drawn with solid lines while calculated parameters are drawn with dashed lines.

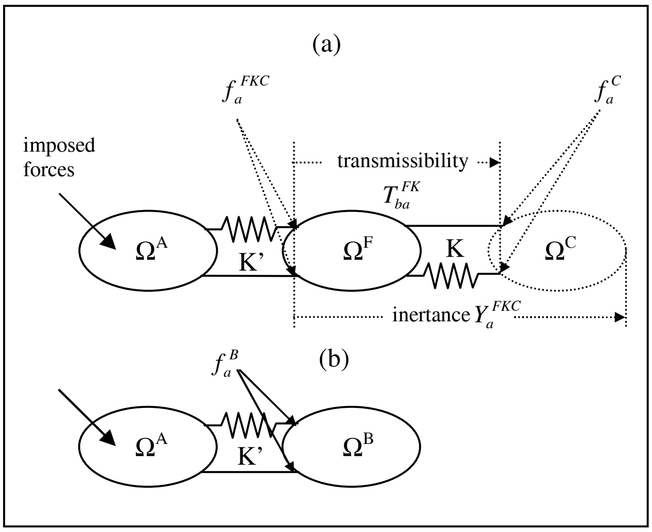

Figure 1: Generic configuration and standard coupling of three structures in series (a) and measurement on a test bench (b).

2.2 Standard coupling of three structures

The procedure presented in this paragraph is standard as all the measured inertance (acceleration/force) matrices concern isolated structures.

If we consider $\Omega^F \cup \Omega^K \cup \Omega^C$ as a new host structure, the forces f_a^{FKC} entering this new host can be predicted from forces measured on the rigid bench by [1]:

$$f_a^{FKC} = \left(-\omega^2 K'^{-1} + Y_b^A + Y_a^{FKC}\right)^{-1}\left(-\omega^2 K'^{-1} + Y_b^A\right) f_a^B, \quad (1)$$

where Y_b^A is the measured inertance matrix of Ω^A, Y_a^{FKC} is the calculated inertance matrix of $\Omega^F \cup \Omega^K \cup \Omega^C$ (Fig. 1) and K' represents the stiffness matrix of the links $\Omega^{K'}$. All the stiffness matrices are given for the application.

The inertance matrix Y_a^{FKC} of $\Omega^F \cup \Omega^K \cup \Omega^C$ can be obtained from isolated structures matrices by:

$$Y_a^{FKC} = Y_a^F - Y_{ab}^F\left(I_a + Y_b^{F^{-1}}\left(Y_a^C - \omega^2 K^{-1}\right)\right)^{-1} Y_b^{F^{-1}} Y_{ba}^F, \quad (2)$$

where $Y^F_{i(i=a,b)}$ are measured submatrices of the inertance matrix of Ω^F, and K represents the stiffness matrix of the links Ω^K.

Then, it is possible to predict f_a^C from f_a^{FKC} by:

$$f_a^C = T_{ba}^{FK} f_a^{FKC}, \tag{3}$$

where T_{ba}^{FK} is a transmissibility matrix given by:

$$T_{ba}^{FK} = \left(Y_b^F + Y_a^C - \omega^2 K^{-1}\right)^{-1} Y_{ba}^F. \tag{4}$$

2.3 Alternative method for coupling three structures in series

The procedure presented in this paragraph is called alternative method as one of the inertance matrices measured concerns two coupled structures: the intermediary and the bench structures.

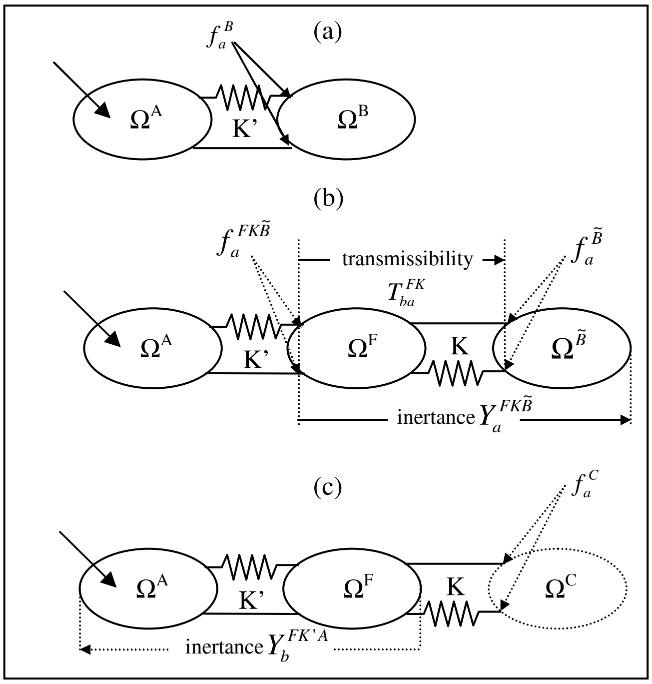

Figure 2: Steps of calculation for the alternative approach.

As for the previous method, the first step consists in measuring forces f_a^B on a rigid bench Ω^B (Fig. 2(a)). Then, as a second step, if we consider $\Omega^A \cup \Omega^{K'} \cup \Omega^F$ as a new source, it is possible to deduce forces $f_a^{\tilde{B}}$ (Fig. 2(b)) entering the test bench from f_a^B by:

$$f_a^{\tilde{B}} = T_{ba}^{FK}\left(-\omega^2 K'^{-1} + Y_b^A + Y_a^{FK\tilde{B}}\right)^{-1}\left(-\omega^2 K'^{-1} + Y_b^A\right) f_a^B, \tag{5}$$

where T_{ba}^{FK} is the transmissibility matrix measured in presence of bench $\Omega^{\tilde{B}}$ and $Y_a^{FK\tilde{B}}$ is the measured inertance matrix of structure $\Omega^F \cup \Omega^K \cup \Omega^{\tilde{B}}$. The last step consists in predicting forces f_a^C from $f_a^{\tilde{B}}$ by:

$$f_a^C = \left(-\omega^2 K^{-1} + Y_b^{FK'A} + Y_a^C\right)^{-1}\left(-\omega^2 K^{-1} + Y_b^{FK'A}\right) f_a^{\tilde{B}}, \tag{6}$$

where the inertance matrix $Y_a^{FK'A}$ is deduced from measured inertance matrices by:

$$Y_a^{FK'A} = Y_b^F - Y_{ba}^F\left(I + Y_a^{F^{-1}}\left(Y_b^A - \omega^2 K'^{-1}\right)\right)^{-1} Y_a^{F^{-1}} Y_{ab}^F. \tag{7}$$

3 Application to a fan system and experimental results

3.1 Industrial configuration and measurements

The two methods are applied in the following industrial case: we consider an engine cooling fan system (EFCS) installed on the chassis of a car (Fig. 3(a)). Source structure Ω^A is the fan system (Fig. 3(b)) while the intermediary structure is the plate on which it is attached (Fig. 3(c)). The vibratory source is a residual unbalance.

The four attachment points between the fan and the plate are elastic while the four attachment points between the plate and the chassis are rigid at the top and elastic at the bottom. Names of attachment points are shown on Fig.3(c) and listed below: BL and BR refer to bottom left and bottom right attach points and TL and TR refer to top left and top right attach point. The frame of reference is the one used in a car and shown on Fig.3. To each attachement point correspond three components of the force vector.

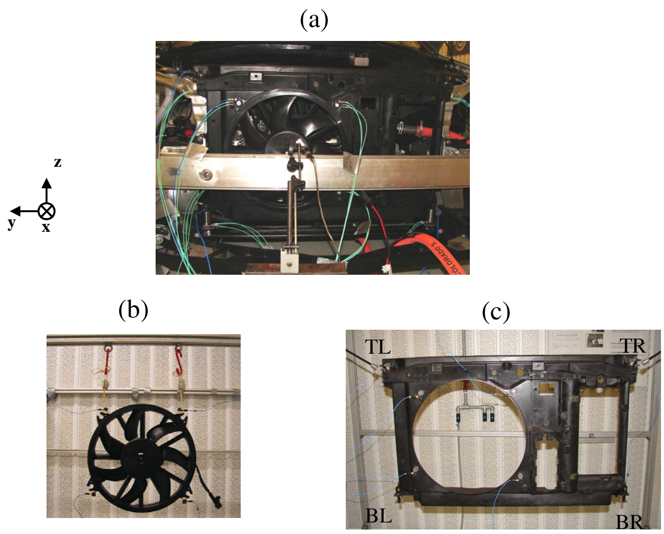

Figure 3: EFCS installed on the chassis of a car (a), fan system (b), plate (c)

The objective consists in predicting the forces entering the chassis (host structure Ω^C) at the plate/chassis interface points from the forces measured on the rigid bench at the fan/plate interface points. To validate the methods, forces entering the chassis are also measured directly.

Forces on the bench and on the chassis are measured by a direct method using force sensors. Terms of inertance and transmissibility matrices are measured using accelerometers and an impact hammer.

3.2 Experimental results

Figure 4 shows six of the twelve predicted and measured forces entering the chassis. Predictions are obtained with the standard and the alternative methods.

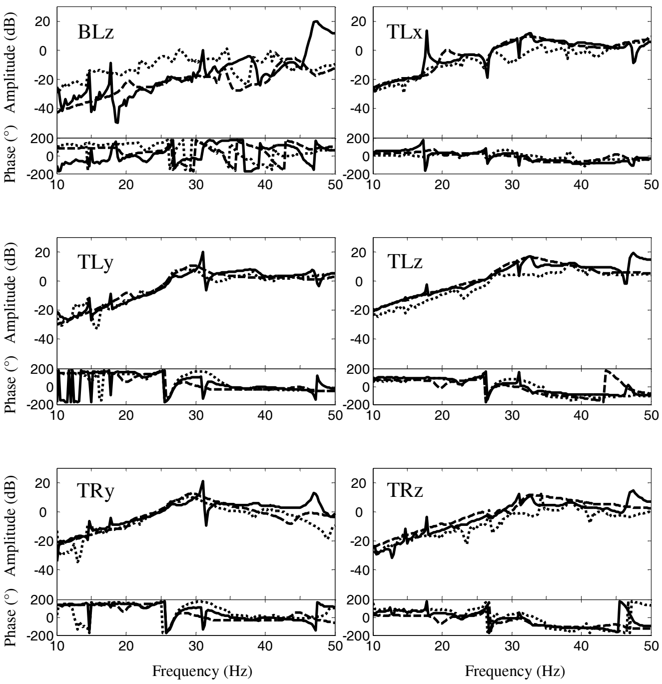

Figure 4: Comparison between predicted and measured forces for three structures in series (--- measured f_a^C , . . . predicted f_a^C with the standard method, ▬ predicted f_a^C with the alternative method).

On one hand, for the standard method, prediction is poor for BLz, TLx, TLz, TRz, and acceptable for TRy between 15 and 45Hz and for TLy. On the other hand, for the alternative method, prediction is acceptable for BLz, TLx, TLz, TRz, good on some frequency bands (TLx, TLy) or very good (TLz). In all cases, results obtained with the alternative method are better than with the standard method.

Using the measured coupling inertance matrix $Y_a^{FK\tilde{B}}$ and the measured coupling transmissibility matrix T_{ba}^{FK} seems to improve the prediction. In theory, results obtained with both methods should be the same. However, it is likely that the use of matrices measured for coupled structures gives more information about coupled degrees of freedom than the use of inertance matrices of isolated structures. This result agrees with results found for an academic case in [4]. Moments and shear forces may act on coupled structures which is not the case on isolated structures [5].

4 Development of a numerical bench

In order to understand which degrees of freedom allow the prediction to be better with the alternative approach, a numerical bench is being developed for academic cases.

This section presents the method developed for the numerical bench for two coupled Euler-Bernoulli beams [2].

4.1 Configuration under study

Figure 5 presents the case under study: we consider a beam A (source beam) attached to a beam C (the host) by one elastic (at $y = y_l$) and one rigid (at $y = y_r$) links. The excitation on the beam A is a force applied at y_s=0.63m. The objective is to predict forces entering the beam C, from forces entering a beam B (the test bench) at connection points.

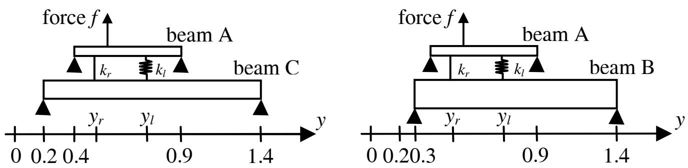

Figure 5: Description of the configurations.

Density and Young modulus for the three beams are: ρ_A = 7800 kg.m^{-3}, ρ_B = 2700 kg.m^{-3}, ρ_C = 7200 kg.m^{-3}, E_A = 2.10^{11}(1+0.05i) Pa, E_B = 0.9.10^{11}(1+0.05i) Pa, E_C = 0.7.10^{11}(1+0.05i) Pa. The rigid link is described by a very high stiffness k_r = 10.10^{10} N.m^{-1} while the elastic link is k_l = 1000 N.m^{-1}. Widths of the beams are: l_A = 2cm, l_B = 8cm and l_C = 5cm. Thicknesses of the beams are: t_A = 2cm, t_B = 20cm and t_C = 5cm The bending coefficient D_i is defined as $D_i = E_i t_i^3 / 12$ for the structure i.

4.2 Method

The basis of the method can be found in [6]. It uses a variational formulation combined with a finite element method.

In this paragraph, the method used to obtain displacements at connection points is described for the coupling of beams A and B. The same method can be used for the coupling of beams A and C.

Displacement ζ_A and ζ_B of beams A and B verify the following differential equations system:

$$\begin{cases} \left(d_y^4 - \gamma_A^4\right)\zeta_A + \dfrac{k_r}{l_A D_A}\left(\zeta_A(y_r) - \zeta_B(y_r)\right) \\ + \dfrac{k_l}{l_A D_A}\left(\zeta_A(y_l) - \zeta_B(y_l)\right) = \dfrac{f}{l_A D_A}\delta(y - y_s), \\ \left(d_y^4 - \gamma_B^4\right)\zeta_B + \dfrac{k_r}{l_B D_B}\left(\zeta_B(y_r) - \zeta_A(y_r)\right) \\ + \dfrac{k_l}{l_B D_B}\left(\zeta_B(y_l) - \zeta_A(y_l)\right) = 0, \end{cases} \quad (8)$$

where γ_i is the bending wave number of the beam i.

The variational formulation of these two equations can be written:

$$\begin{cases} \int_0^{L_A} \delta\zeta_A \left(\frac{k_r}{l_A D_A} (\zeta_A(y_r) - \zeta_B(y_r)) + \frac{k_l}{l_A D_A} (\zeta_A(y_l) - \zeta_B(y_l)) \right) dy \\ + \int_0^{L_A} \frac{d^2(\delta\zeta_A)}{dy^2} \frac{d^2\zeta_A}{dy^2} dy - \gamma_A^4 \int_0^{L_A} \delta\zeta_A . \zeta_A dy = \int_0^{L_A} \delta\zeta_A . \frac{f}{l_A D_A} \delta(y - y_s) dy, \\ \int_0^{L_B} \delta\zeta_B \left(\frac{k_r}{l_B D_B} (\zeta_B(y_r) - \zeta_A(y_r)) + \frac{k_l}{l_B D_B} (\zeta_B(y_l) - \zeta_A(y_l)) \right) dy \\ + \int_0^{L_B} \frac{d^2\delta\zeta_B}{dy^2} \frac{d^2\zeta_B}{dy^2} dy - \gamma_B^4 \int_0^{L_B} \delta\zeta_B . \zeta_B dy = 0, \end{cases} \quad (9)$$

with $\delta\zeta_A$, resp. $\delta\zeta_B$, the virtual variation of ζ_A, resp. ζ_B.

Previous equations are discretized and the interpolation functions given in [6] are used to solve the problem. Then Eq. (9) is written in a matrix form:

$$\begin{bmatrix} A & F \\ E & B \end{bmatrix} \begin{Bmatrix} u_A \\ u_B \end{Bmatrix} = \begin{Bmatrix} f_A \\ 0 \end{Bmatrix}, \quad (10)$$

where

$$A = K_A - \gamma_A^4 M_A + \begin{array}{c} \begin{array}{cc} \zeta_A(y_r) \text{ column} & \zeta_A(y_l) \text{ column} \end{array} \\ \begin{bmatrix} 0 & \cdots & 0 & \cdots & 0 & 0 \\ \vdots & \ddots & 0 & \cdots & 0 & \vdots \\ \vdots & & \frac{k_r}{l_A D_A} & & 0 & \vdots \\ \vdots & & 0 & \ddots & 0 & \vdots \\ \vdots & \cdots & 0 & \cdots & \frac{k_l}{l_A D_A} & \vdots \\ 0 & \cdots & 0 & \cdots & 0 & 0 \end{bmatrix} \end{array} \begin{array}{l} \\ \\ \delta\zeta_A(y_r) \text{ line} \\ \\ \delta\zeta_A(y_l) \text{ line} \\ \\ \end{array},$$

$$E = \begin{array}{c} \begin{array}{cc} \zeta_A(y_r) \text{ column} & \zeta_A(y_l) \text{ column} \end{array} \\ \begin{bmatrix} 0 & \cdots & 0 & \cdots & 0 & 0 \\ \vdots & \ddots & 0 & \cdots & 0 & \vdots \\ \vdots & & -\frac{k_l}{l_B D_B} & & & \vdots \\ \vdots & & 0 & \ddots & 0 & \vdots \\ \vdots & \cdots & & \cdots & -\frac{k_r}{l_B D_B} & \vdots \\ 0 & \cdots & 0 & \cdots & 0 & 0 \end{bmatrix} \end{array} \begin{array}{l} \\ \\ \delta\zeta_B(y_r) \text{ line} \\ \\ \delta\zeta_B(y_l) \text{ line} \\ \\ \end{array}.$$

Matrices B and F can be written the same way. Matrix K_A is the stiffness matrix of beam A while matrix M_A is the mass matrix of beam A. Their expressions can be found in [6].

Terms of vectors u_A and u_B are displacements and rotations at nodes and vector f_A is the force vector.

Terms of vectors u_B can be found by solving Eq. (10):

$$u_B = \left(E A^{-1} F - B \right)^{-1} E A^{-1} f_A \quad . \quad (11)$$

Displacements $\zeta_B(y_l)$ and $\zeta_B(y_r)$ at the two connection points can be extracted from vector u_B. Then forces $f_B(y_l)$ and $f_B(y_r)$ entering the beam B at connection points can be calculated.

4.3 Validation

Recall of the modal method

Results obtained with the finite element method are compared with results obtained by a modal method described in this paragraph.

We consider two beams S_1 and S_2 coupled by one elastic and one rigid connections; a force f_0 is applied on beam S_1 (Fig. 6). Displacements ζ_1 and ζ_2 at connection points 1 and 2 can be written

$$\begin{cases} \zeta_1(\omega) = \alpha_{10}^{(1)}(\omega) f_0 + \alpha_{11}^{(1)}(\omega) f_1 + \alpha_{12}^{(1)}(\omega) f_2 \\ \zeta_2(\omega) = \alpha_{20}^{(1)}(\omega) f_0 + \alpha_{21}^{(1)}(\omega) f_1 + \alpha_{22}^{(1)}(\omega) f_2 \end{cases} \quad (12)$$

where

$$\alpha_{ij}(\omega) = \alpha(y_i, y_j, \omega) = \frac{\zeta(y_i, y_j, \omega)}{f_j} = \sum_{n-1}^{\infty} \frac{\Psi_n(y_i)\Psi_n(y_j)}{\omega_n^2 - \omega^2}$$

is the receptance and Ψ_n is the n[th] eigenmode of the beam.

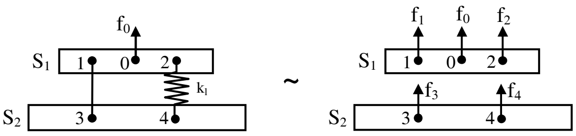

Figure 6: Beams connected by elastic and rigid links

In a matrix form, Eq.(12) is:

$$T_{12} \begin{Bmatrix} f_1 \\ \zeta_1 \end{Bmatrix} = \begin{Bmatrix} f_2 \\ \zeta_2 \end{Bmatrix} + \begin{Bmatrix} \beta_1 \\ \beta_2 \end{Bmatrix} f_0 \quad (13)$$

where

$$\beta_1 = \frac{\alpha_{10}^{(1)}}{\alpha_{12}^{(1)}}, \beta_2 = \frac{\alpha_{22}^{(1)}\alpha_{10}^{(1)}}{\alpha_{12}^{(1)}} - \alpha_{20}^{(1)}, T_{12} = \begin{bmatrix} -\frac{\alpha_{11}^{(1)}}{\alpha_{22}^{(1)}} & \frac{1}{\alpha_{12}^{(1)}} \\ \alpha_{21}^{(1)} - \frac{\alpha_{11}^{(1)}\alpha_{22}^{(1)}}{\alpha_{12}^{(1)}} & \frac{\alpha_{22}^{(1)}}{\alpha_{12}^{(1)}} \end{bmatrix}.$$

In the same way, displacements ζ_3 and ζ_4 at connection points 3 and 4 on beam S_2 can be written:

$$T_{34} \begin{Bmatrix} f_3 \\ \zeta_3 \end{Bmatrix} = \begin{Bmatrix} f_4 \\ \zeta_4 \end{Bmatrix} \text{ where } T_{34} = \begin{bmatrix} -\frac{\alpha_{33}^{(2)}}{\alpha_{44}^{(1)}} & \frac{1}{\alpha_{34}^{(2)}} \\ \alpha_{43}^{(2)} - \frac{\alpha_{33}^{(2)}\alpha_{44}^{(2)}}{\alpha_{34}^{(2)}} & \frac{\alpha_{44}^{(2)}}{\alpha_{34}^{(2)}} \end{bmatrix}. \quad (14)$$

At elastic and rigid links, displacement and forces are linked by:

$$T_{13} \begin{Bmatrix} f_1 \\ \zeta_1 \end{Bmatrix} = \begin{Bmatrix} f_3 \\ \zeta_3 \end{Bmatrix} \text{ and } T_{24} \begin{Bmatrix} f_2 \\ \zeta_{21} \end{Bmatrix} = \begin{Bmatrix} f_4 \\ \zeta_4 \end{Bmatrix} \quad (15)$$

where

$$T_{13} = \begin{bmatrix} -1 & 0 \\ 0 & 1 \end{bmatrix} \text{ and } T_{24} = \begin{bmatrix} -1 & 0 \\ 1/k & 1 \end{bmatrix}$$

are respectively the transfer matrices between points 1 and 3 and between points 2 and 4.

Then, it is possible to find the displacement and the force at point 1 with:

$$\left(T_{12} - T_{24}^{-1}T_{34}T_{13}\right)\begin{Bmatrix} f_1 \\ \zeta_1 \end{Bmatrix} = \begin{Bmatrix} \beta_1 \\ \beta_{21} \end{Bmatrix} f_0 . \qquad (16)$$

Displacements and forces at other points are deduced using Eq. (14) and Eq. (15).

Results for free acceleration

Results are presented on Figure 7 for the free acceleration of beam A at rigid and elastic points. Free acceleration a_f of beam A can be calculated from forces entering beams B and C by:

$$a_{fB} = \left(-\omega^2 K^{-1} + Y^A + Y^B\right) f^B ,$$
$$a_{fC} = \left(-\omega^2 K^{-1} + Y^A + Y^C\right) f^C ,$$

where Y^A, Y^B and Y^C are inertance matrices of beams A, B and C at connection points.

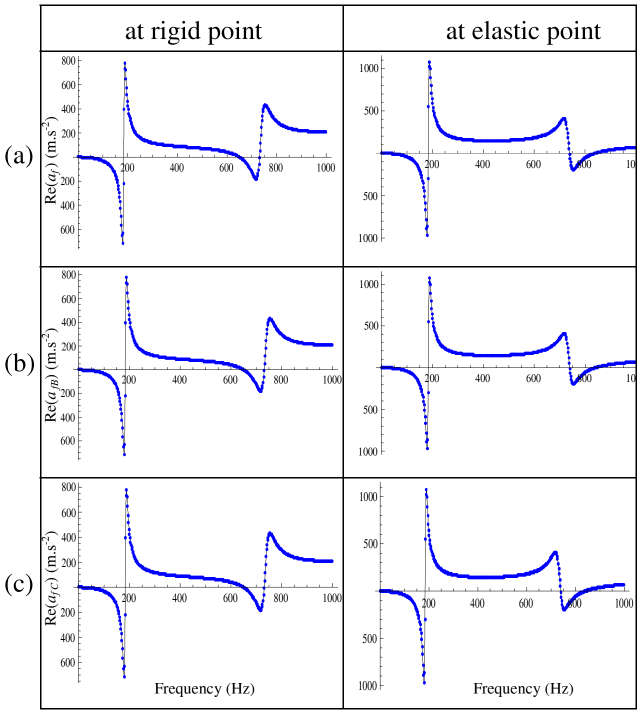

Figure 7: Real part of free acceleration of beam A calculated directly (a), calculated from the coupling on bench B (b), calculated from the coupling on host C (c) (▬ modal method, ●—● EF method)

Firstly, the EF method is validated as it gives exactly the same results as the modal method. Secondly, whichever method is used (direct method or via a host structure), results for free acceleration are similar. These results confirm that the method of prediction of forces on a host structure from measurement of forces on another structure give the same exact results in theory.

5 Conclusion

In the industrial studied case, two methods to predict forces at connection points between two structures have been shown: the first one uses only parameters measured for isolated structures while the second one uses some parameters of coupled structures. The prediction is better with the second method. More information on coupled degrees of freedom seems to be given by coupled structures than isolated ones.

In order to understand why the second method gives better result a numerical bench has been developed. The case of two beams coupled by one rigid and one elastic connection points has been studied. The numerical bench has been validated with a comparison of the results obtained by a modal method. Moreover, results showed that in theory, the prediction of forces on the host structure should be exactly the same as the measurements on the host structure.

The next step is now to use the numerical bench with three structures coupling in series in order to understand which coupled degrees of freedom allow to obtain better results in the prediction.

References

[1] V. Martin, M.-H. Moulet, S. Mapagha, "Prediction of forces applied on a receiver by two vibrating structures installed in series; Application to an engine cooling fan mounted on a car chassis", *Acta Acustica United with Acustica* 97, 877-889 (2011)

[2] V. Martin and A. Pasqual, "Rapport du contrat IACV", *Rapport interne*, 8 Juin 2011.

[3] W. Liu, D. J. Ewins, "Substructure synthesis via elastic media", *Journal of Sound and Vibration*, 257, 361-379 (2002)

[4] A. Elliott, A. T. Moorhouse, "Characterisation of structure borne sound sources from measurements in-situ", *Proceedings Congress Acoustics 08*, Paris, 2008

[5] A. T. Moorhouse, T. A. Evans, A. S. Elliott, "Some relationships for coupled structures and their application to measurement of structural dynamic properties *in situ*", Mechanical Systems and Signal Processing, 25, 1574-1584 (2011)

[6] V. Martin, "Éléments d'acoustique générale", Presses Polytechniques et Universitaires Romandes, 2007.